COBEM 2021 Florianópolis - Brasil
ABCM Associação Brasileira de Engenharia e Ciências Mecânicas
26th ABCM International Congress of Mechanical Engineering
November 22-26, 2021. Florianópolis, SC, Brazil

COB-2021-0385
Uncertainty Propagation and Reliability Analysis of Conventional and Tow-Steered Composite Plates

Henrique E. A. A. dos Santos
Leandro R. Cunha
Domingos A. Rade
Aeronautics Institute of Technology, Praça Mal. Eduardo Gomes 50, Vila das Acácias, São José dos Campos, São Paulo, Brazil, 12228-900
henriqueheaas@ita.br
lrcunha@ita.br
rade@ita.br

Abstract. *The uncertainty propagation and reliability analysis of conventional and tow-steered composite laminate plates subjected to various sources of uncertainties are numerically investigated in this paper. A model based on the Rayleigh-Ritz approach with the hypotheses of the Classical Lamination Theory is proposed to incorporate uncertainties affecting the following: the lamina fiber volume, which is modeled as a two-dimensional random field described by the Karhunen-Loève Expansion; the boundary conditions, where discrete springs are modeled as random variables; and some specific parameters of fiber trajectory definition, which are also modeled as random variables. By considering the behavior of rectilinear and curvilinear fiber laminates in terms of linear buckling loads, the Monte Carlo Simulation (MCS) is used for uncertainty propagation and the reliability assessment is performed with the first-order reliability method (FORM) and also with MCS for a conventional and two tow-steered composite laminates with optimized fiber trajectories. The reliability results are compared and accurate results from FORM are observed with a significant reduction of computational costs. Additionally, the presented incorporation and quantification of uncertainties indicate the benefits of fiber steering technology and seem to be useful in designing real composite structures.*

Keywords: *tow-steered laminates, uncertainty quantification, reliability, buckling.*

1. Introduction

In the past decades, the development of automated methods for manufacturing composites, such as Automated Fiber Placement (AFP), has enabled the emergence of an alternative to standard unidirectional fiber laminates: the tow-steered or variable angle tow (VAT) laminate, a type of variable stiffness composite laminate (VSCL) where the fibers are put curvilinearly in the lamina following a specific trajectory (Ribeiro *et al.*, 2014).

Although the possibility of greater design space with mitigated stress concentrations favors the use of VAT laminates, the production of curvilinear fibers is an additional source of uncertainties for composite materials, which are already affected by a range of variabilities. Due to the random nature of the material and the complexity in manufacturing process, considerable uncertainties can arise from voids and variations in volume fractions of fibers and matrix, imperfections in bonding between components, damage and misalignment in fibers, residual stresses, temperature effects, non-uniform curing process, and others. These uncertainties propagate to a larger scale, which increases the variability in overall stiffness and strength of the material (Zhou *et al.*, 2017).

Sriramula and Chryssanthopoulos (2009) compiled in a review paper different modeling techniques for uncertainty propagation, which are described according to the type of starting model scale of the aleatory uncertainty, namely, micro-scale, meso-scale, and macro-scale. There are a variety of works which have studied the propagation of uncertainties in composite laminates, from the propagation on structural responses, such as maximum displacement and critical Tsai number (António and Hoffbauer, 2008), to the use of polynomial chaos expansion (PCE) to predict aeroelastic responses (Guimarães *et al.*, 2020; Manan and Cooper, 2009).

In the context of structural analyses in the presence of uncertainties, a particular interest is oriented towards the estimation of structural reliability, understood as the probability that a given structural system will perform satisfactorily under determined circumstances. Several works related to reliability analyses in composites have been published in the last decades, with the first contributions found in (Cederbaum *et al.*, 1990), where the effect of randomness in static loads is investigated considering the Hashin failure criterion as the performance function, and in (Soares, 1997), where the reliability of the laminate is explored by its modeling as a system of laminas in series or in parallel. Comparison

between reliability analysis methods when considering composite materials has also been conducted, mainly by verifying the agreement between the first-order reliability method (FORM) and the Monte Carlo Simulation (MCS) (Lekou and Philippidis, 2008; Sciuva and Lomario, 2003).

Particularly regarding reliability of VSCL, less numerous but very important works have been conducted. In (Sohouli *et al.*, 2017), by varying the standard deviation of random variables, reliability analyses of curvilinear and straight fiber composites showed that the curved fiber plate presented considerably lower probability of failure in both considered criteria, tip deflection and first ply failure. In a different approach, the reliability of VSCL was guaranteed in (Sohouli *et al.*, 2018) by the reliability-based design optimization.

The characterization of a system performance under the presence of uncertainties can be represented by the so-called limit state function (LSF), a limit in the design space formed by a set of random variables that separates the region on which the structure satisfies the adopted criteria from the region where such a condition does not hold. In this study, the LSF analyzed is related to a design criterion of great importance to structural components subjected to compressive or shear loads: the buckling resistance. Studies have demonstrated considerable improvements in buckling capacity when using tow-steered composites (Hyer and Lee, 1991; Wu *et al.*, 2012), with an increase of up to 35.8% in buckling load limit (Lopes *et al.*, 2008).

Based on the context presented, this paper aims to conduct uncertainty propagation and reliability assessment of conventional (straight fiber) and tow-steered composite plates regarding their linear buckling behavior in the presence of uncertainties, which are assumed to affect the lamina properties, boundary conditions, and manufacturing tolerances.

A more comprehensive investigation, which considers, in addition to the LSF related to buckling, two others related to the fundamental natural frequency and critical flutter speed of VAT composite plates, can be found in (Santos, 2021).

2. Formulation

2.1 Plate Model

A rectangular tow-steered composite laminate plate with dimensions a x b is represented in Fig. 1, where the axes X and Y are the laminate global directions, and the plane xy represents the lamina local directions oriented for each ply according to the angle ϕ_i between directions X and x. The variation of fiber orientation angle $\theta(x, y)$ in each lamina is defined based on (Wu *et al.*, 2012) according to the following equation, with the Lagrangian polynomials representing the distribution and the fiber angle values T_{mn} being chosen at predefined reference points (x_m, y_n):

$$\theta(x,y) = \phi_i + \sum_{m=0}^{M-1}\sum_{n=0}^{N-1} T_{mn} \prod_{m\neq k}\left(\frac{x-x_k}{x_m-x_k}\right)\prod_{n\neq j}\left(\frac{y-y_j}{y_n-y_j}\right) . \tag{1}$$

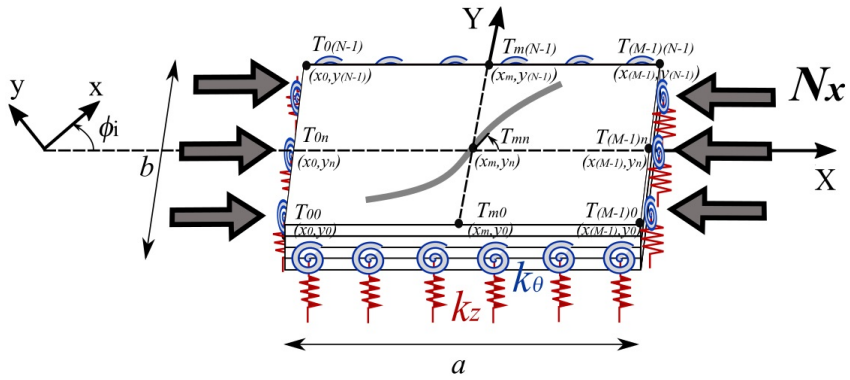

Figure 1. A rectangular tow-steered composite laminate plate with fiber angle values T_{mn} at reference points. Also, it is indicated the discrete translational and torsional springs and compressive load. Based on (Wu *et al.*, 2012).

It is worth mentioning that a specific stacking sequence is considered in this work as a base configuration for the laminate, where laminas of the same thickness and same fiber trajectory are stacked following the angle-ply of the sequence (angle ϕ_i in Eq. 1).

By assuming the hypotheses of the CLT and considering only symmetric laminates (without membrane-bending coupling), besides neglecting any stretching in the middle plane of the laminate, it is possible to write the strain energy U of the plate as (Reddy, 2007):

$$U = \frac{1}{2}\int_{-a/2}^{a/2}\int_{-b/2}^{b/2} \boldsymbol{\kappa}^T(x,y)\boldsymbol{D}(x,y)\boldsymbol{\kappa}(x,y)\, dydx , \tag{2}$$

where $\boldsymbol{\kappa}(x,y)$ is the vector of middle-surface curvatures and $\boldsymbol{D}(x,y)$ is the bending stiffness matrix.

The Rayleigh-Ritz method is used to approximate the plate transverse displacement field w_0 in terms of normalized coordinates $\zeta = 2x/a$ and $\eta = 2y/b$ using the Legendre polynomials as follows (Wu *et al.*, 2012):

$$w_0(\zeta,\eta) = \boldsymbol{F}(\zeta,\eta)\boldsymbol{A} = (1-\zeta^2)^c(1-\eta^2)^c \sum_{i=0}^{I}\sum_{j=0}^{J} X_i(\zeta)Y_j(\eta)A_{ij} \ , \tag{3}$$

where $c = 0, 1,$ or 2, for free, simply supported, and clamped edges boundary conditions, respectively, $\boldsymbol{A} = \{A_{ij}\}$ represents the generalized coordinates, and the functions $X_i(\zeta)$ and $Y_j(\eta)$ are defined as:

$$X_i(\zeta) = \frac{1}{2^i}\sum_{k=0}^{i}\binom{i}{k}^2 (\zeta-1)^{i-k}(\zeta+1)^k \quad ; \quad Y_j(\eta) = \frac{1}{2^j}\sum_{k=0}^{j}\binom{j}{k}^2 (\eta-1)^{j-k}(\eta+1)^k \ .$$

Translational and torsional springs will be used to model the non ideal clamped condition applied along all the edges of the plate and, consequently, Eq. 3 is used with $c = 0$ and the boundary condition is represented by the complementary strain energy of the springs at the four edges. The formulations of these energies are written for translational and torsional springs, respectively, as:

$$\begin{aligned} Uz = \frac{1}{2}\Bigg[&\int_{-b/2}^{b/2} k_z \left(w_0|_{x=\frac{-a}{2}}\right)^2 dy + \int_{-b/2}^{b/2} k_z \left(w_0|_{x=\frac{a}{2}}\right)^2 dy \\ &+ \int_{-a/2}^{a/2} k_z \left(w_0|_{y=\frac{-b}{2}}\right)^2 dx + \int_{-a/2}^{a/2} k_z \left(w_0|_{y=\frac{b}{2}}\right)^2 dx \Bigg] \ , \end{aligned} \tag{4}$$

$$\begin{aligned} U_\theta = \frac{1}{2}\Bigg[&\int_{-b/2}^{b/2} k_\theta \left(\left.\frac{\partial w_0}{\partial x}\right|_{x=\frac{-a}{2}}\right)^2 dy + \int_{-b/2}^{b/2} k_\theta \left(\left.\frac{\partial w_0}{\partial x}\right|_{x=\frac{a}{2}}\right)^2 dy \\ &+ \int_{-a/2}^{a/2} k_\theta \left(\left.\frac{\partial w_0}{\partial y}\right|_{y=\frac{-b}{2}}\right)^2 dx + \int_{-a/2}^{a/2} k_\theta \left(\left.\frac{\partial w_0}{\partial y}\right|_{y=\frac{b}{2}}\right)^2 dx \Bigg] \ , \end{aligned} \tag{5}$$

where k_z and k_θ are the stiffness per unit length of translational and torsional springs, respectively.

Then, the total strain energy is computed as:

$$U_T = U + Uz + U_\theta \ .$$

The potential energy V of an external uniaxial compressive load applied in the plate, with a force per unit length N_x, can be written as (Timoshenko and Gere, 1989):

$$V = -\frac{1}{2}\int_{-a/2}^{a/2}\int_{-b/2}^{b/2} N_x \left(\frac{\partial w_0}{\partial x}\right)^2 dydx \ . \tag{6}$$

By applying the principle of minimum total potential energy considering the expressed for U_T and V, with the displacement field w_0 in Eq. 3 and the necessary adjustments concerning the transformation to normalized coordinates ζ and η, the following eigenvalue problem for buckling analysis is obtained:

$$\left(\boldsymbol{K_S} + \boldsymbol{K} - N_x\, \boldsymbol{K_N}\right)\boldsymbol{A} = \boldsymbol{0} \ , \tag{7}$$

where $\boldsymbol{K_S}$ is the spring stiffness matrix, $\boldsymbol{K}$ is the structural stiffness matrix, $\boldsymbol{K_N}$ is the modified geometric stiffness matrix, and N_x is the eigenvalue vector of compressive buckling loads.

2.2 Discretization of Random Field by KLE

The lamina mechanical properties can be determined from the contributions of fiber and matrix volume fractions according to the rule of mixture, which is omitted here and can be found in (Agarwal *et al.*, 2006).

Based on the work conducted in (Guimarães *et al.*, 2020), the lamina fiber volume is represented by a two-dimensional stationary random field as:

$$V_f(\zeta,\eta,\Theta) = \bar{V}_f + \Delta V_f(\zeta,\eta,\Theta) = \bar{V}_f + \sum_{n=1}^{M_k}\sqrt{\lambda_n}\xi_n(\Theta)f_n(\zeta,\eta), \tag{8}$$

where $\bar{V}_f$ is the mean of fiber volume, Θ belongs to the space of random events, and the variation ΔV_f is expressed according to KLE approach, where M_k is the number of terms in the truncated series expansion, ξ_n is a set of independent Gaussian random variables with zero mean, and the eigenvalues λ_n and eigenvectors f_n are the solutions of the integral equation associated with the covariance function. By assuming an exponential covariance function of a two-dimensional domain, the integral eigenvalue problem to be solved can be written as below:

$$\int_{-1}^{1}\int_{-1}^{1} e^{-|\zeta_1-\zeta_2|/l_\zeta-|\eta_1-\eta_2|/l_\eta} f(\zeta_2,\eta_2)d\zeta d\eta = \lambda_n f_n(\zeta_1,\eta_1)\ ,\ \ n=1,...,M_k\ \ , \tag{9}$$

where l_ζ and l_η are the correlation lengths in the ζ and η directions, respectively. In this work, they will be both considered equal 1.0. The solution of Eq. 9 above is found in details in (Ghanem and Spanos, 1991).

2.3 Reliability Methods

2.3.1 Hasofer-Lind / FORM

The Hasofer-Lind (H-L) method is a type of FORM applicable for normal random variables where the limit state function is represented by the first-order Taylor series expansion at the most probable point (MPP) of failure. By using g to denote the limit state function (LSF) of n independent random variables normally distributed and gathered in vector $\boldsymbol{X} = [X_1\ X_2\ ...\ X_n]$, where this function indicates the safe ($g > 0$) and unsafe ($g < 0$) regions, it is possible to define the following with R representing the resistance of the structure and S the demand:

$$g(\boldsymbol{X}) = R(\boldsymbol{X}) - S(\boldsymbol{X})\ . \tag{10}$$

As required by the method, the random variables are transformed into their standardized (reduced) forms as follows:

$$X_i' = \frac{X_i - \mu_{X_i}}{\sigma_{X_i}}\ \ (i=1,2,...,n), \tag{11}$$

where μ_{X_i} and σ_{X_i} are the mean and standard deviation of X_i, respectively. Then, the mean and standard deviation of X_i' are, respectively, zero and unity.

The shortest distance in the standard normalized coordinate system from the origin to the design point, or MPP, on the limit state surface $g = 0$ is a measure of reliability and, therefore, is defined as the reliability index β_{HL}. In the case of nonlinear limit state functions, β_{HL} can be determined by solving the following optimization problem:

$$\begin{aligned} &\text{Minimize: } \sqrt{(\boldsymbol{X'})^T\ \boldsymbol{X'}} \\ &\text{Subjected to: } g(\boldsymbol{X'}) = 0\ . \end{aligned} \tag{12}$$

In order to obtain β_{HL} and the coordinates of MPP, Hasofer and Lind (1974) formulated an algorithm which can also be found in details in (Choi *et al.*, 2007) and is omitted here.

Considering the property of rotational symmetry of the standard normal probability density function, the failure probability P_f can be calculated with the cumulative distribution function (CDF) of standard normal distribution, which leads to the following reliability expression:

$$R_\beta = 1 - P_f = 1 - \boldsymbol{\Phi}\left(-\beta_{HL}\right)\ . \tag{13}$$

2.3.2 Monte Carlo Simulation

The Monte Carlo Simulation (MCS) is a simple and powerful tool which can be, in many cases, computationally expensive due to a high number of simulation cycles required according to the necessary accuracy.

After the generation of random values according to the distribution type of each random variable, the limit state function is evaluated for each sample set of random variables and the reliability can be estimated as:

$$R_{MCS} = 1 - P_f \approx 1 - \frac{n_f}{N}\ , \tag{14}$$

where N is the number of simulation cycles and n_f is the number of times $g(\boldsymbol{X}) < 0$ (failures) in the simulation.

3. Numerical applications

3.1 Model description

In the numerical applications of this work, the conventional and tow-steered composite laminate plates are of length (a) 400mm and width (b) 300mm, where laminæ of thickness 0.19mm follow the stacking sequence $[0°/\text{-}45°/45°/90°]_s$,

which determines the angle ϕ_i of local directions. In the specific case of tow-steered laminates, the laminæ have their fiber trajectories defined by Eq. 1.

The mechanical properties of fiber and matrix are found in Table 1. The mean value $\bar{V}_f$ adopted is 0.60.

Table 1. Mechanical properties of fiber and matrix.

Material	E (GPa)	G (GPa)	ν	ρ (kg/m^3)
Fiber (AS)*	231	15	0.2	1790
Matrix (Epoxy I)*	3.2	1.2	0.35	1272

* Data from (Kaddour and Hinton, 2012), except the density data.

Two convergence analyses are deterministically carried out before starting the study with uncertainties. The first one aims at choosing the necessary number of functions in Eq. 3 to guarantee a satisfactory convergence of the critical buckling load N_1, the lowest value of N_x obtained from Eq. 7. By choosing a high value of stiffness per unit length for the translational and torsional springs, i.e., $k_z = 10^9 N/mm^2$ and $k_\theta = 10^9 N/rad$, and setting the same number of functions in the x and y expansion directions, the evolution of the critical buckling load with the increase of functions in the Rayleigh-Ritz approach for the conventional laminate is showed in Table 2, where it is considered $I = J = 8$ sufficient to guarantee a good convergence. This consideration is kept for all the subsequent computations.

Table 2. Critical buckling loads for different number of functions in the Rayleigh-Ritz approach.

Critical Buckling Load	I = J					
	5	6	7	8	9	10
N_1 (N/mm)	16.596	15.412	15.396	15.362	15.361	15.360

The second convergence analysis refers to the determination of k_z and k_θ. The influence of these parameters is assessed in order to choose values which are not exceedingly large to reach stable responses, being able to notice their influences in further analysis involving uncertainties. Figure 2 shows the evolution of critical buckling load for the conventional laminate in order to determine k_z (Fig. 2 (a)), where by keeping $k_\theta = 0$ the boundary condition tends to the simply-supported one, and to determine k_θ (Fig. 2 (b)), where by keeping $k_z = 10^9 N/mm^2$ the boundary condition approaches the clamped one. By selecting the values of 1.5 N/mm^2 and 500 N/rad for k_z and k_θ, respectively, the variation of these stiffness parameters in the stochastic analyses can still be verified. These values will also be used in all the subsequent applications.

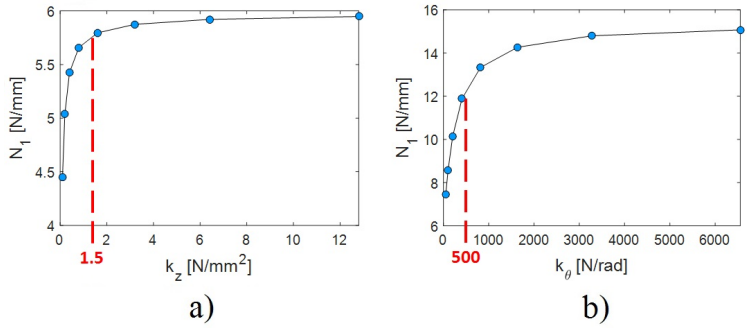

Figure 2. Evolution of critical buckling load for the determination of k_z (a) and k_θ (b).

3.2 Optimization

In this work, a GA algorithm from the commercial software Matlab is used for the optimization of fiber trajectories of VAT plates to maximize the critical buckling load N_1. The trajectory parameters T_{mn} defined in Eq. 1 are the design variables and the optimization problem is formulated as:

$$\begin{aligned} &\text{Maximize: } N_1 \\ &\text{Design variables: } [T_{00}..T_{mn}] \\ &\text{Subjected to: } -\pi/2 \leq T_{mn} \leq \pi/2 \end{aligned} \tag{15}$$

Two different configurations of fiber trajectory for VAT plates are considered to perform the optimization: 4 design variables T_{mn} chosen at the corners of the plate, labeled as *4V*; and 9 design variables T_{mn} chosen at equally spaced points of the plate, labeled as *9V*. The optimized fiber trajectories are shown in Fig. 3 and the optimum fiber angles are presented in Table 3 with the critical buckling load obtained for each configuration. Also in Table 3, it can be found the results for the conventional laminate, labeled as *C*, for the sake of comparison.

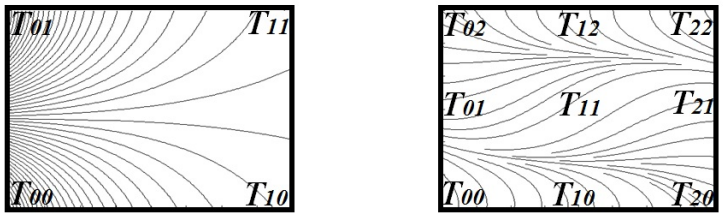

Figure 3. Optimized fiber trajectories for the configurations *4V* (a) and *9V* (b).

Table 3. Results of the conventional laminate and the two optimized configurations for tow-steered laminates.

Configuration	Optimized angles T_{mn}	N_1 (N/mm)
C	-	11.85
4V	$T_{01} = 89.91^\circ$; $T_{11} = 59.49^\circ$ $T_{00} = -75.11^\circ$; $T_{10} = -50.90^\circ$	12.84
9V	$T_{02} = -36.42^\circ$; $T_{12} = -89.98^\circ$; $T_{22} = -60.63^\circ$ $T_{01} = 0.80^\circ$; $T_{11} = 34.99^\circ$; $T_{21} = 1.92^\circ$ $T_{00} = -89.30^\circ$; $T_{10} = -89.64^\circ$; $T_{20} = -35.95^\circ$	13.69

3.3 Uncertainty Propagation

The uncertainties incorporated in the analysis are those related to the lamina fiber volume, the boundary conditions and the parameters of fiber trajectory. The KLE is used to represent the lamina fiber volume as a two-dimensional random field $V_f(\zeta, \eta, \Theta)$, according to Eq. 8, which requires the choice of M_k terms in the truncated series expansion representing the variation. Since the resulting eigenvalues solution of the Eq.9 are computed and sorted in descending order, it is identified the largest of them to keep only the most influential ones in the expansion. This procedure led to conclude that M_k=8 is satisfactory.

Hence, the following quantities are considered as independent and normally distributed random variables: the first eight zero-mean ξ_n from Eq. 8; the stiffnesses per unit length k_z and k_θ; and the fiber angles T_{mn}. The standard deviation of the random variables are varied with the use of three different values of coefficient of variation (COV), which is the ratio of the standard deviation to the mean.

Two important considerations about the calculation of standard deviation are necessary: since the mean of the first eight ξ_n are zero, their standard deviations were obtained by using as mean the same value of $\bar{V}_f$, which is 0.60; and as the uncertainties in manufacturing are related to the accuracy of processes and techniques, independently of the angle value, it was used the same mean to obtain the standard deviation of all fiber angle random variables, which is 90° (the modulus of the maximum allowed value). The stiffnesses k_z and k_θ had their standard deviations calculated with their own mean values. Table 4 summarizes the mean and standard deviations used for random variables.

The impact of the uncertainties is characterized for the 3 configurations (C, 4V, and 9V), where for the conventional laminate (C), one random variable T_{mn} with zero mean is considered, such that $\theta = \phi_i + T_{mn}$. For each configuration and each COV, the MCS method combined with the Latin Hypercube Sampling (LHS) is used to generate 10,000 samples of random variables to compute, for each set, the critical buckling load from Eq. 7.

From the results depicted in Fig. 4, it is possible to verify that the distributions obtained for all responses are approximately symmetric, with values of skewness (lack of symmetry about the mean) between -0.03 and 0.02, and normal, with values around 3 for kurtosis (referring to the tails of the distribution). In addition, there seems to be a quasi-linear relationship between the values of COV of the input variables with those of the output variables.

Table 4. Mean values and standard deviations of all random variables according to the coefficient of variation considered.

Random Variable	Mean Value	Standard Deviation		
		COV=0.01	COV=0.05	COV=0.10
ξ_1	0	0.006	0.030	0.060
ξ_2	0	0.006	0.030	0.060
ξ_3	0	0.006	0.030	0.060
ξ_4	0	0.006	0.030	0.060
ξ_5	0	0.006	0.030	0.060
ξ_6	0	0.006	0.030	0.060
ξ_7	0	0.006	0.030	0.060
ξ_8	0	0.006	0.030	0.060
k_z (N/mm^2)	1.5	0.015	0.075	0.150
k_θ (N/rad)	500	5	25	50
$[T_{00}..T_{mn}]$ ($^\circ$)	*	0.9	4.5	9.0

* The mean values of fiber angles are the optimized angles for configurations 4V and 9V (Table 3) and 0° for configuration C.

3.4 Reliability Analysis

The reliability analysis is conducted by using the same independent and normally distributed random variables presented in Table 4. The LSF associated to buckling is defined with deterministic demand and random resistance as:

$$g_B(\boldsymbol{X}) = N_1(\boldsymbol{X}) - 0.95 \cdot N_1(\mu_X) \,, \tag{16}$$

where $N_1(\mu_X)$ is obtained from Eq. 7 with the mean values of random variables as input, using a factor of 0.95 to constitute the demand, and the random response $N_1(\boldsymbol{X})$ is also from Eq. 7.

Considering different values of COV, the H-L method is used to compute the reliability R_β for configurations C, 4V, and 9V regarding LSF from Eq. 16, as described in subsection 2.3.1 The gradient components required by the method are approximated with finite differences.

The evolution of reliability with the increase of COV of input random variables for the three configurations is shown in Fig. 5. The results of reliability are practically the same for all configurations, indicating equal influence on their critical buckling load when increasing the uncertainties.

3.4.1 Sensitivity Analysis

The relative contribution of each random variable on the variation of reliability can be quantified by the sensitivity factor α_i. In a sensitivity analysis, the following property by squaring the sensitivity factors can be used:

$$\sum_{i=1}^{N_V} \alpha_i^2 = \sum_{i=1}^{N_V} \left(- \frac{\dfrac{\partial g(\boldsymbol{x'^*})}{\partial X_i} COV \mu_{X_i}}{\sqrt{\displaystyle\sum_{i=1}^{N_V} \left(\frac{\partial g(\boldsymbol{x'^*})}{\partial X_i} COV \mu_{X_i} \right)^2}} \right)^2 = 1 \,, \tag{17}$$

where α_i is not dependent of COV, as demonstrated.

The squared sensitivity factors of all random variables in the reliability analysis are shown in a bar graph in Fig. 6 for each configuration. The similar results of reliability for all configurations can be explained by the enormous contribution of ξ_1, which accounts for more than 70% of influence on reliability results of the three configurations. Particularly interesting to notice are the low contributions of random variables associated to fiber angles, where it can be inferred that uncertainties in fiber trajectories have very small influence on the reliability.

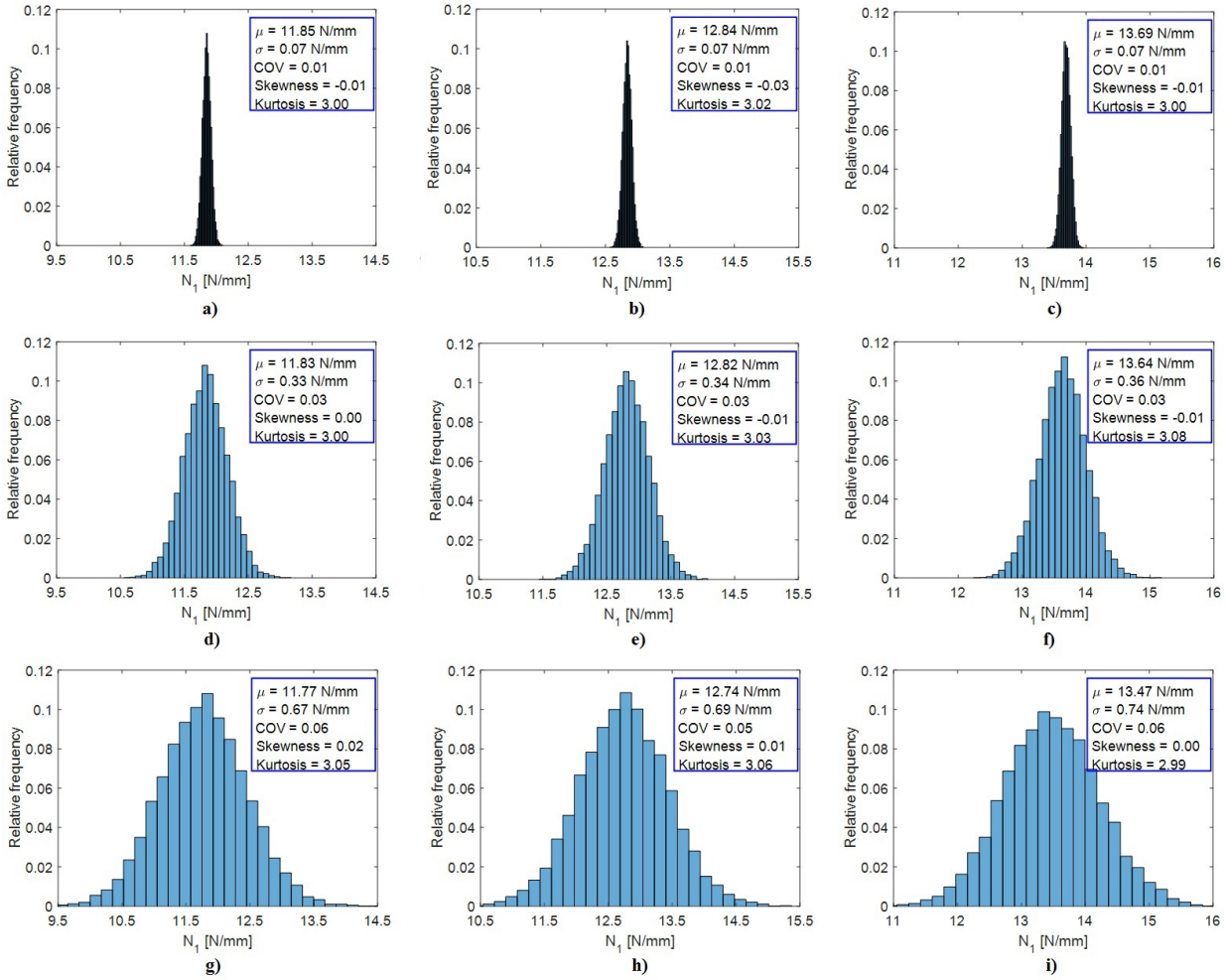

Figure 4. Histograms of critical buckling load distributions for configurations C (a,d,g), 4V (b,e,h), and 9V (c,f,i) in ascending order of COV used, which are 0.01, 0.05, and 0.10.

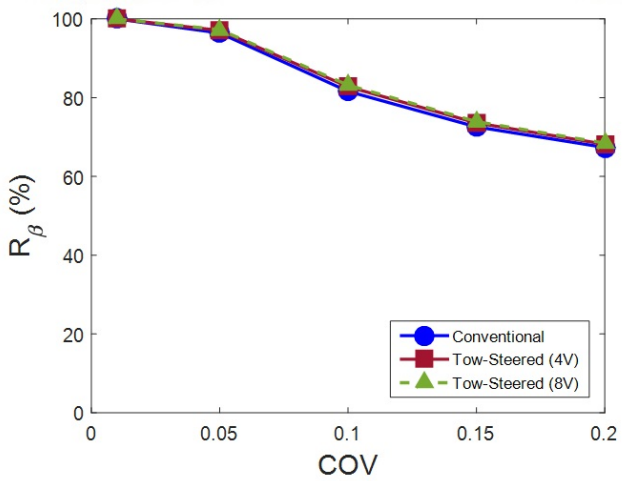

Figure 5. The reliability R_β resulting from the H-L method for different values of COV.

3.4.2 Hasofer-Lind Method Validation

Some values of reliability from the H-L method are chosen to be compared with their counterparts from the MCS, which has been performed with 10,000 sets of samples of random variables generated with the LHS method. A machine of 3.60GHz processor and 16GB of RAM is used for both methods of simulation.

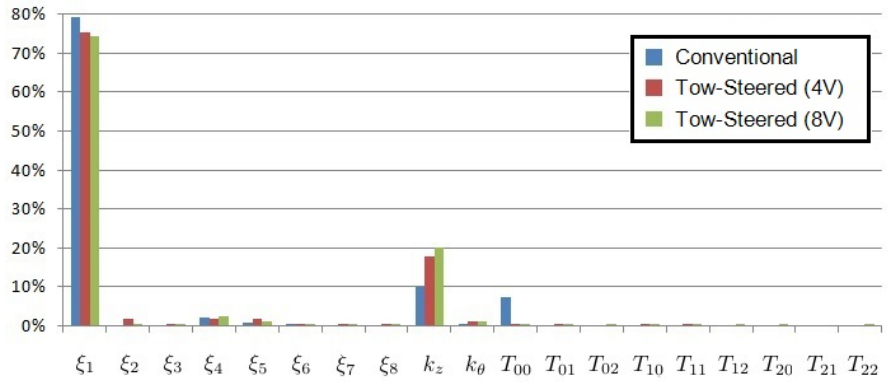

Figure 6. Squared sensitivity factors of each random variable regarding the reliability analysis.

From Table 5, it is observed, in general, small differences. Since the H-L method is exact for independent normally distributed random variables, as considered in this work, and for linear limit state functions, the low nonlinearity of the limit state functions can account for the small deviations, especially for low values of COV. Besides the good degree of accuracy, with the exception of the configuration 9V with COV equals 0.10, the H-L method have demonstrated to be significantly more efficient, with considerably lower time consumption.

Table 5. Comparison of reliability results from H-L and MCS methods.

COV		Config. C		Config. 4V		Config. 9V	
		H-L	MCS	H-L	MCS	H-L	MCS
0.01	Reliability	100.00%	100.00%	100.00%	100.00%	100.00%	100.00%
	Time	00h13m31s	11h34m38s	00h16m16s	12h17m26s	00h22m36s	17h12m51s
	Difference	0.00%		0.00%		0.00%	
0.05	Reliability	96.42%	95.77%	97.07%	96.27%	97.28%	95.60%
	Time	00h12m54s	11h34m21s	00h16m18s	12h21m58s	00h22m54s	16h42m23s
	Difference	0.67%		0.83%		1.76%	
0.10	Reliability	81.61%	77.99%	82.78%	78.34%	83.20%	72.85%
	Time	00h12m33s	11h59m15s	00h16m23s	13h05m11s	00h22m59s	16h47m12s
	Difference	4.64%		5.67%		14.20%	

4. Conclusions

This paper aimed at numerically investigating conventional and tow-steered laminate plates subjected to uncertainties affecting the material properties, boundary conditions, and manufacturing tolerances in the production of fiber trajectories. A stochastic structural model is constructed based on the Rayleigh-Ritz method with the hypotheses of the Classical Lamination Theory, which is combined with the KLE for the discretization of the two-dimensional random field for modeling the lamina fiber volume, enabling the uncertainty propagation and reliability assessment with te use of MCS and H-L methods.

The optimization of fiber trajectories of VAT plates conducted with a GA algorithm demonstrated the capability of tow-steering technology for improving critical buckling load of composite laminates, although the best result obtained is related to an unfeasible configuration due to the complexity of the trajectory for current manufacturing limitations.

Results of uncertainty propagation and reliability analysis comparing a conventional laminate with two optimized tow-steered laminates did not demonstrate significant differences, even with the increase of random variables when using more complex trajectories, indicating that inaccuracies of fiber trajectories have small influence on reliability. In addition, the accuracy and efficiency of H-L method could also be verified, where small differences in general and orders of magnitude

lower time consumption were obtained when comparing with MCS.

Therefore, the results presented in this work can contribute with the growing interest involving the tow-steering technology considering the involved uncertainties. Future works including optimization constraints could better explore the benefits of fiber steering.

5. ACKNOWLEDGEMENTS

D.A. Rade acknowledges the support provided by the São Paulo Research Foundation - FAPESP (grant #2018/15894-0) and the Brazilian Research Council (CNPq) (grants #310633/2013-3 and #312068/2020-4).

6. REFERENCES

Agarwal, B.D., Broutman, L.J. and Chandrashekhara, K., 2006. *Analysis and Performance of Fiber Composites*. John Wiley & Sons, Inc., 3rd edition.

António, C.C. and Hoffbauer, L.N., 2008. "From local to global importance measures of uncertainty propagation in composite structuress". *Composite Structures*, Vol. 85, pp. 213–225.

Cederbaum, G., Elishakoff, I. and Librescu, L., 1990. "Reliability of laminated plates via the First-Order Second-Moment method". *Composite Structures*, Vol. 15, pp. 161–167.

Choi, S.K., Grandhi, R.V. and Canfield, R.A., 2007. *Reliability-based Structural Design*. Springer, London.

Ghanem, R.G. and Spanos, P.D., 1991. *Stochastic Finite Elements: A Spectral Approach*. Springer-Verlag New York Inc., New York.

Guimarães, T.A.M., Silva, H.L., Rade, D.A. and Cesnik, C.E.S., 2020. "Aeroelastic stability of conventional and tow-steered composite plates under stochastic fiber volume". *AIAA Journal, American Institute of Aeronautics and Astronautics*, Vol. X, pp. 1–12.

Hasofer, A.M. and Lind, N.C., 1974. "Exact and invariant second moment code format". *Journal of the Engineering Mechanics Division*, Vol. 100, pp. 111–121.

Hyer, M. and Lee, H., 1991. "The use of curvilinear fiber format to improve buckling resistance of composite plates with central circular holes". *Composite Structures*, Vol. 18, pp. 239–261.

Kaddour, A.S. and Hinton, M.J., 2012. "Input data for test cases used in benchmarking triaxial failure theories of composites". *Journal of composite materials*, Vol. 46, pp. 2295–2312.

Lekou, D. and Philippidis, T., 2008. "Mechanical property variability in FRP laminates and its effect on failure prediction". *Composites: Part B*, Vol. 39, pp. 1247–1256.

Lopes, C., Gürdal, Z. and P.P.Camanho, 2008. "Variable-stiffness composite panels: Buckling and first-ply failure improvements over straight-fibre laminates". *Composite Structures*, Vol. 86, pp. 897–907.

Manan, A. and Cooper, J., 2009. "Design of composite wings including uncertainties: A probabilistic approach". *Journal of Aircraft*, Vol. 46, No. 2, pp. 601–607.

Reddy, J.N., 2007. *Theory and Analysis of Elastic Plates and Shells*. CRC Press LLC, Boca Raton, Florida, 2nd edition.

Ribeiro, P., Akhavan, H., Teter, A. and Warmiński, J., 2014. "A review on the mechanical behaviour of curvilinear fibre composite laminated panels". *Journal of Composite Materials*, Vol. 48, No. 22, pp. 2761–2777.

Santos, H.E.A.A., 2021. *Reliability Analysis of Tow-Steered Composite Laminate Plates*. Master of Science in Aeronautical and Mechanical Engineering, Instituto Tecnológico de Aeronáutica, São José dos Campos.

Sciuva, M.D. and Lomario, D., 2003. "A comparison between monte carlo and FORMs in calculating the reliability of a composite structure". *Composite Structures*, Vol. 59, pp. 155–162.

Soares, C.G., 1997. "Reliability of components in composite materials". *Reliability Engineering & System Safety*, Vol. 55, pp. 171–177.

Sohouli, A., Yildiz, M. and Suleman, A., 2017. "Design optimization and reliability analysis of variable stiffness composite structures". *In: Smart Structures and Materials*, Vol. 43, pp. 245–265.

Sohouli, A., Yildiz, M. and Suleman, A., 2018. "Efficient strategies for reliability-based design optimization of variable stiffness composite structures". *Structural and Multidisciplinary Optimization*, Vol. 57, pp. 689–704.

Sriramula, S. and Chryssanthopoulos, M.K., 2009. "Quantification of uncertainty modelling in stochastic analysis of FRP composites". *Composites: Parte A*, Vol. 40, pp. 1673–1684.

Timoshenko, S.P. and Gere, J.M., 1989. *Theory of elastic stability*. Dover Publications, Inc., New York, 2nd edition.

Wu, Z., Weaver, P., Raju, G. and Kim, C., 2012. "Buckling analysis and optimisation of variable angle tow composite plates". *Thin-Walled Structures*, Vol. 60, pp. 163–172.

Zhou, X.Y., Gosling, P., Ullah, Z., Kaczmarczyk, L. and Pearce, C., 2017. "Stochastic multi-scale finite element based reliability analysis for laminated composite structures". *Applied Mathematical Modelling*, Vol. 45, pp. 457–473.

7. RESPONSIBILITY NOTICE

The authors are solely responsible for the printed material included in this paper.